Syntheses and Magnetic Properties of Layered $LnSrMn_{0.5}Ni_{0.5}O_4$ (Ln = La, Pr, Nd, Sm, Gd) Compounds

Kunpyo Hong,[†] Young-Uk Kwon,*[,†] Duk-Kyun Han,[†] Jeong-Soo Lee,[‡] and Sung-Hyun Kim[§]

Department of Chemistry, Sungkyunkwan University, Suwon, 440-746, Korea, Korea Atomic Energy Research Institute, Taejon, 350-600, Korea, and Department of Chemistry, Konkuk University, Seoul, 143-701, Korea

Received February 16, 1999. Revised Manuscript Received April 14, 1999

K_2NiF_4-type layered compounds $LnSrMn_{0.5}Ni_{0.5}O_4$ (Ln = La, Pr, Nd, Sm, Gd) were synthesized, and their magnetic properties were studied. Both Curie−Weiss fits and X-ray absorption near-edge structure (XANES) of Mn and Ni atoms indicate that the oxidation states of Mn and Ni are +4 and close to +2, respectively. The oxidation state of Ni is assigned primarily as Ni^{II}, although there is increasing contribution from Ni^{III} as the size of Ln increases. These compounds show overall antiferromagnetic behavior in their magnetic susceptibility vs temperature plots. The data in the paramagnetic regions indicate that there are ferromagnetic contributions by showing positive Weiss temperatures, probably because the Mn^{IV} and Ni^{II} atoms are locally ordered to form ferromagnetic regions. The antiferromagnetic behavior of the La compound is attributed to the interactions among these ferromagnetic regions within the MO_2 (M = Mn, Ni) layers. In the Pr and Nd compounds, there are additional local maxima at lower temperatures that are attributed to the interlayer antiferromagnetic ordering between the ferromagnetic regions and the Pr/Nd ions. Low-temperature neutron diffraction data of Pr and Nd samples show a magnetic Bragg peak that is absent in the La sample. The Sm and Gd compounds show still different behaviors from the La−Nd compounds that can be explained with the reduced interlayer interactions due to the small ionic sizes and the different magnetic properties of Sm and Gd ions.

Introduction

B-site mixed perovskite oxides of the general formula $LnMn_{0.5}M_{0.5}O_3$ (Ln = rare earths, M = Co, Ni, Cu) have attracted continued interest over decades because these compounds are ferromagnetic while the parent perovskite compounds are either antiferromagnetic or Pauli paramagnetic.[1] In fact, this group of compounds constitutes a rare class of ferromagnetic perovskite oxides along with the colossal magnetoresistance $Ln_{1-x}A_xMnO_3$ (A = divalent cations)[2] and $SrRuO_3$[3] while most of the other perovskites are antiferromagnetic or paramagnetic. However, the details of the electronic states of the metal ions and the mechanism of the ferromagnetism remain controversial.[4−10]

The evolution of the physical properties with the dimensionality of the structure is another important theme in solid-state science. Therefore, there has been much effort to synthesize 2D Ruddelsden−Popper $((AO)(ABO_3)_n$, $n = 1, 2, ...)$ type compounds to compare with the 3D perovskites for the physical properties.[11,12]

We have been interested in whether the ferromagnetic nature of the perovskite compounds $LnMn_{0.5}Ni_{0.5}O_3$ can be maintained if their 2D derivatives are formed. Very recently, Millburn et al. reported on $LaSrMn_{0.5}Ni_{0.5}O_4$ compound in the $n = 1$ K_2NiF_4 structure (Figure 1) for the synthesis and magnetic properties.[13] Contrary to the analogous perovskite $LaMn_{0.5}Ni_{0.5}O_3$, this compound exhibits an antiferromagnetic ordering. On the basis of the magnetic measurements and the crystal structure analysis as compared with that of $LaSrCr_{0.5}Ni_{0.5}O_4$, they claimed to observe high spin Ni^{III} ions in their compound.

We have extended their studies by substituting La with other rare earths. In this paper, we report our results on B-site mixed $LnSrMn_{0.5}Ni_{0.5}O_4$ (Ln = La, Pr, Nd, Sm, and Gd) compounds for the synthesis, structure, and magnetic properties.

* Corresponding author.
[†] Sungkyunkwan University.
[‡] Korea Atomic Energy Research Institute.
[§] Konkuk University.

(1) Blasse, G. J. *Phys. Chem. Solids* **1965**, *26*, 1969.
(2) Wollan, E. O.; Koehler, W. C. *Phys. Rev.* **1955**, *100*, 545.
(3) Jonker, G. H. *Physica* **1956**, *22*, 707.
(4) Rao, C. N. R.; Cheetham, A. K.; Mahesh, R. *Chem. Mater.* **1996**, *8*, 2421 and references therein.
(5) Longo, J. M.; Raccah, P. M.; Goodenough, J. B. *J. Appl. Phys.* **1968**, *39*, 1327.
(6) Sonobe, M.; Kichizo, A. *J. Phys. Soc. Jpn.* **1992**, *61*, 4193.
(7) Asai, K.; Sekizawa, H.; Iida, S. *J. Phys. Soc. Jpn.* **1979**, *47*, 1054.
(8) Vasanthacharya, N. Y.; Singh, K. K.; Ganguly, P. *Rev. Chim. Miner.* **1981**, *18*, 333.
(9) Sarma, D. D.; Rader, O.; Kachel, T.; Chainani, A.; Mathew, M.; Holldack, K.; Gudat, W.; Eberhardt, W. *Phys. Rev. B* **1994**, *49*, 14238.
(10) Vasanthacharya, N. Y.; Ganguly, P.; Goodenough, J. B.; Rao, C. N. R. *J. Phys. C: Solid State Phys.* **1984**, *17*, 2745.
(11) Moritomo, Y.; Asamitsu, A.; Kawahara, H.; Tokura, Y. *Nature* **1996**, *380*, 141.
(12) Nozaki, A.; Yoshikawa, H.; Wada, T.; Yamauchi H.; Tanaka, S. *Phys. Rev. B* **1991**, *43*, 181.
(13) Millburn, J. E.; Rosseinsky, M. J. *J. Mater. Chem.* **1998**, *8*, 1413.

10.1021/cm990098k CCC: $18.00
Published on Web 06/09/1999

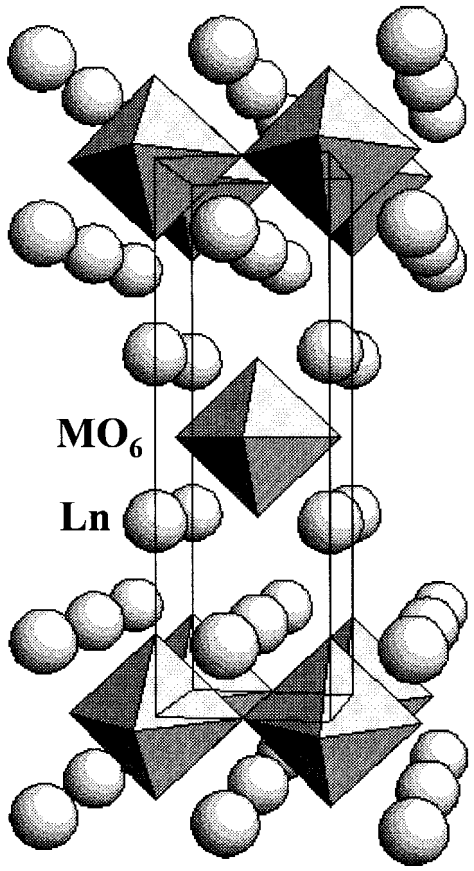

Figure 1. Crystal structure of K_2NiF_4-type $LnSrMn_{0.5}Ni_{0.5}O_4$ (Ln = La, Pr, Nd, Sm, Gd).

Experimental Section

Single-phase samples of the title compounds were synthesized from the conventional solid-state reaction method. Stoichiometric amounts of R_2O_3 (R = La, Nd, Sm, Gd), Pr_6O_{11}, $MnCO_3$, and NiO were ground together, pressed into pellets, and heated at 1400 °C for 24 h in air. All the reagents were baked overnight before use.

Room temperature powder neutron diffraction experiments for La-, Pr-, and Nd-containing compounds were performed with a HRPD in the research reactor, HANARO, which is located at Korea Atomic Energy Research Institute (KAERI). The wavelength of 1.8339 Å was selected with a Ge(331) monochromator, which is vertically bent. The data were collected in the 2θ range of 0−160° with 0.05° steps. A vanadium can with 0.1 mm thickness was used to reduce noise. The detector efficiency was corrected based on a separate experimental result. Rietveld pattern refinements on the powder patterns were performed with the Fullprof program.[14] Absorption corrections were applied according to the formalism by Hewat.[15] The background was fitted with a polynomial function with six parameters. The peak shape was described by a four-term pseudo-Voigt function including an isotropic strain parameter, a four-term asymmetric peak shape function, and a modified March's function for preferred orientation.

Magnetic measurements were performed on a SQUID in the temperature range of 5−300 K for both field-cooled (FC) and zero-field-cooled (ZFC) runs under 100 and 5000 G magnetic field strengths. The samples were placed in a capsule and cooled to 5 K with and without an applied field, and the measurements were made while warming the samples.

XANES measurements in a transmission mode were carried out at line 3C1 of Pohang light source (PLS) and line 7C of photon factory (PF), operating at an energy of 2.05 and 2.5 GeV with a ring current of ca. 100−200 and 200−400 mA, respectively. The monochromatic beam was obtained by a Si(111) double crystal that was detuned by 30% to reject higher harmonics. In the XANES region, the energy was scanned with an increment of 0.3 eV. The vertical slit width was adjusted less than 1 mm for a better energy resolution. The energy calibration was done using metallic foils of three-absorption length. The first inflection points were taken as E_0 (6539 eV for Mn and 8333 eV for Ni) and used to calibrate all the data.

(14) Rodriguez-Carvajal, J. *Fullprof*, Version 3.2; Jan97-LLB-JRC; Laboratoire Leon Brillouin (CEA-CNRS): 1997.
(15) Hewat, A. W. *Acta Crystallogr. A* **1979**, *35*, 248.

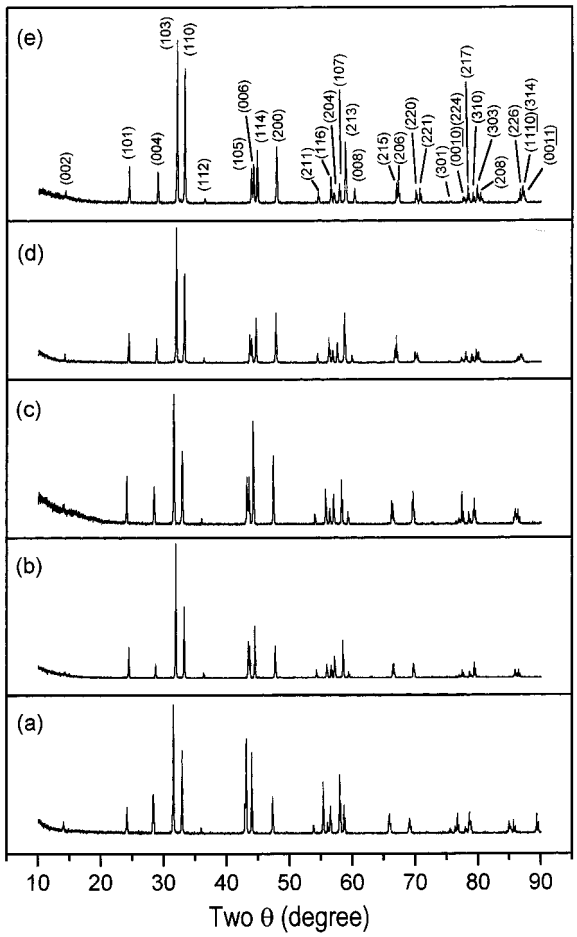

Figure 2. X-ray powder diffraction patterns of $LnSrMn_{0.5}Ni_{0.5}O_4$: Ln = (a) La, (b) Pr, (c) Nd, (d) Sm, and (e) Gd.

Table 1. Lattice Parameters for $LnSrMn_{0.5}Ni_{0.5}O_4$ (Ln = La, Pr, Nd, Sm, Gd)

Ln	La[a]	Pr[a]	Nd[a]	Sm[b]	Gd[b]
a	3.8377(5)	3.8155(1)	3.8095(4)	3.8075(7)	3.800(3)
c	12.566(2)	12.452(1)	12.410(2)	12.358(2)	12.290(9)
V	185.07(5)	181.28(2)	180.10(4)	179.16(6)	177.5(2)

[a] From Rietveld refinements of powder neutron diffraction data. [b] From least squares refinements of powder X-ray diffraction peak positions.

Results and Discussion

The title compounds were synthesized as single phases in the ideal tetragonal K_2NiF_4-type structure, based on their powder X-ray diffraction patterns (Figure 2) from the conventional solid-state reactions at 1400 °C in air. The lattice parameters of the compounds, listed in Table 1, increase almost linearly with the increase of the ionic radius of Ln. However, in their paper, Millburn et al. discussed the difficulty of obtaining a pure $LaSrMn_{0.5}Ni_{0.5}O_4$ sample free of perovskite

Table 2. Rietveld Profile Refinements of the Powder Neutron Diffraction Data for $LnSrMn_{0.5}Ni_{0.5}O_4$ (Ln = La, Pr, Nd) at 300 K

atom[a]		La	Pr	Nd
Ln/Sr	z	0.3599(2)	0.3595(2)	0.3597(1)
	B_{iso}	0.49(7)	0.33(8)	0.30(7)
	occu	0.97(1)	0.95(1)	0.99(1)
Mn/Ni	B_{iso}	1.5(2)	1.2(2)	1.1(2)
	occu	0.94(3)	0.96(3)	0.94(3)
O1	B_{iso}	0.70(7)	0.95(6)	0.61(7)
	occu	0.98(1)	1.00(1)	0.98(1)
O2	z	0.1656(2)	0.1676(2)	0.1679(2)
	B_{iso}	1.32(8)	1.40(7)	1.39(8)
	occu	1	1	1
R_p		7.29	5.83	5.64
R_{wp}		8.72	7.80	7.52
χ^2		1.41	1.95	2.23

[a] Atomic positions: Ln/Sr, 0,0,z; Mn/Ni, 0,0,0; O1, 0,1/2,0; O2, 0,0,z.

impurity when the sample was prepared in either air or pure oxygen. Therefore, they prepared their samples by a low-temperature decomposition reaction of a nitrate solution and subsequent heat treatments at 1200 and 1300 °C under dried and deoxygenated argon. They attributed the difficulty to the thermodynamics of the oxygen-containing system, which favored the formation of perovskite phases.[13] The different synthesis results between ours and in the literature appear to be due to the different reaction temperatures. Apparently, the $LaSrMn_{0.5}Ni_{0.5}O_4$ phase is unstable at 1200 °C but is stable at 1400 °C in air, and probably the same is true for the other compounds with different Ln atoms. Ganguly et al. also reported their synthesis of $LaSrMn_{0.5}Ni_{0.5}O_4$ compound from a solid-state reaction at 1200 °C in air but without any comment on the sample purity.[16]

To observe the possible superstructure due to Mn and Ni ordering, the La, Pr, and Nd samples were submitted to neutron diffraction studies to take advantage of the large difference of the neutron scattering lengths for Mn (-0.3730×10^{-12} cm) and Ni (1.0300×10^{-12} cm). There was no sign of superstructure formation in the powder patterns in agreement with the electron diffraction studies on the La compound in the literature, which also did not reveal any sign of superstructure.[13] The Rietveld profile refinements with the K_2NiF_4-type ($I4/mmm$, no. 139) structures were performed on these diffraction data, and the results are summarized in Table 2. The calculated and observed powder patterns are shown in Figure 3. The refined parameters for the La compound agree with the X-ray data in the literature.[13] Important bond distances and angles are given in Table 3. The M−O bonds in the c-direction ($M-O_{ax}$) are slightly longer than those in the ab-plane ($M-O_{eq}$) implying a tetragonal distortion. The $M-O_{ax}/M-O_{eq}$ ratio are calculated to be 1.085, 1.090, and 1.087 for the La, Pr, and Nd compounds, respectively. These are slightly larger than those reported for the La compounds (1.069 and 1.073 from the 1200 and 1300 °C syntheses, respectively). However, since powder X-ray Rietveld refinements usually have large uncertainties in oxygen parameters, these differences may not be meaningful.

(16) Ganguly, P.; Vasanthacharya, N. Y.; Rao, C. N. R.; Edwards, P. P. *J. Solid State Chem.* **1984**, *54*, 400.

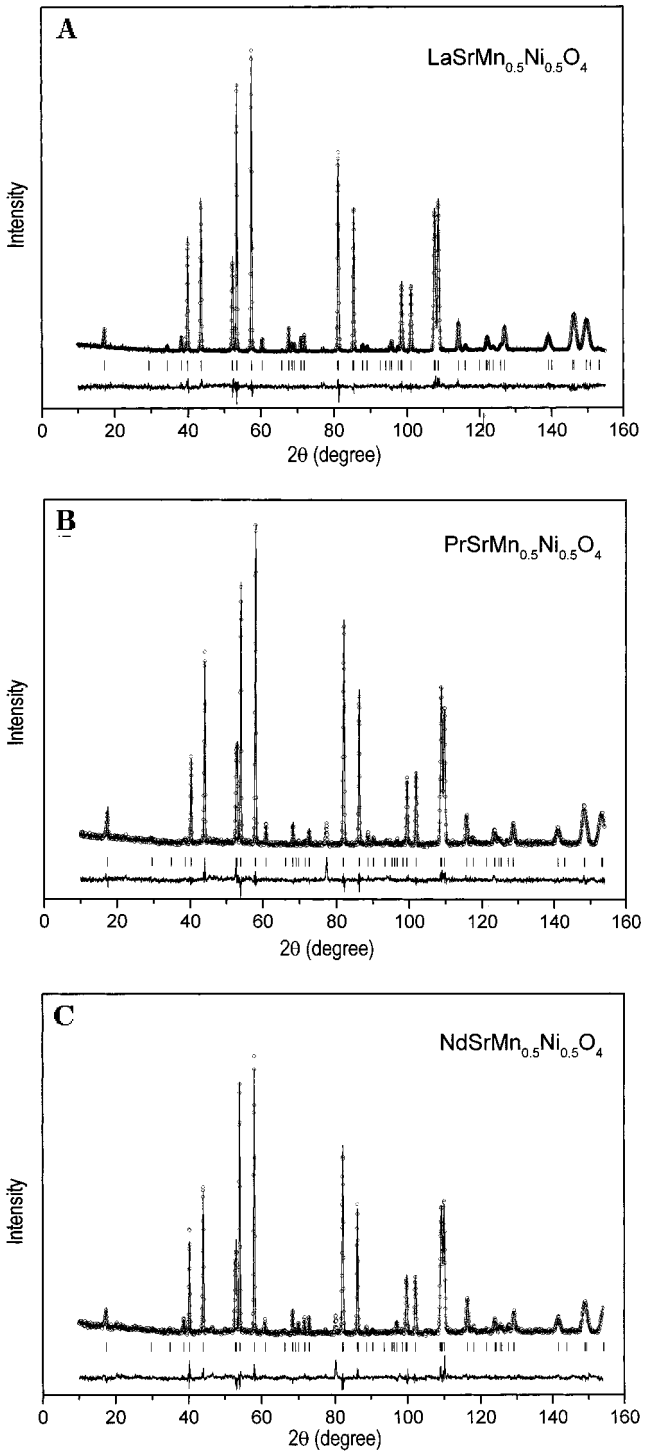

Figure 3. Neutron powder diffraction patterns for $LnSrMn_{0.5}Ni_{0.5}O_4$ compounds at room temperature: Ln = (A) La, (B) Pr, and (C) Nd. The observed and calculated data are shown as open circles and solid lines, and the peak positions are shown by the tick marks. The difference between the observed and calculated patterns are shown as solid lines at the bottom. The peaks at $2\theta = 77-80°$ are due to the sample container and are excluded in the refinements.

The magnetic susceptibility data of $LnSrMn_{0.5}Ni_{0.5}O_4$ compounds are shown in Figure 4. All of the compounds show local maxima at 105−126 K, indicating antiferromagnetic interactions. The paramagnetic data of the $1/\chi$ vs T plots deviate from the Curie−Weiss law by showing concave up curvatures. We have tried to get straight lines by including χ_{TIP} and diamagnetic correc-

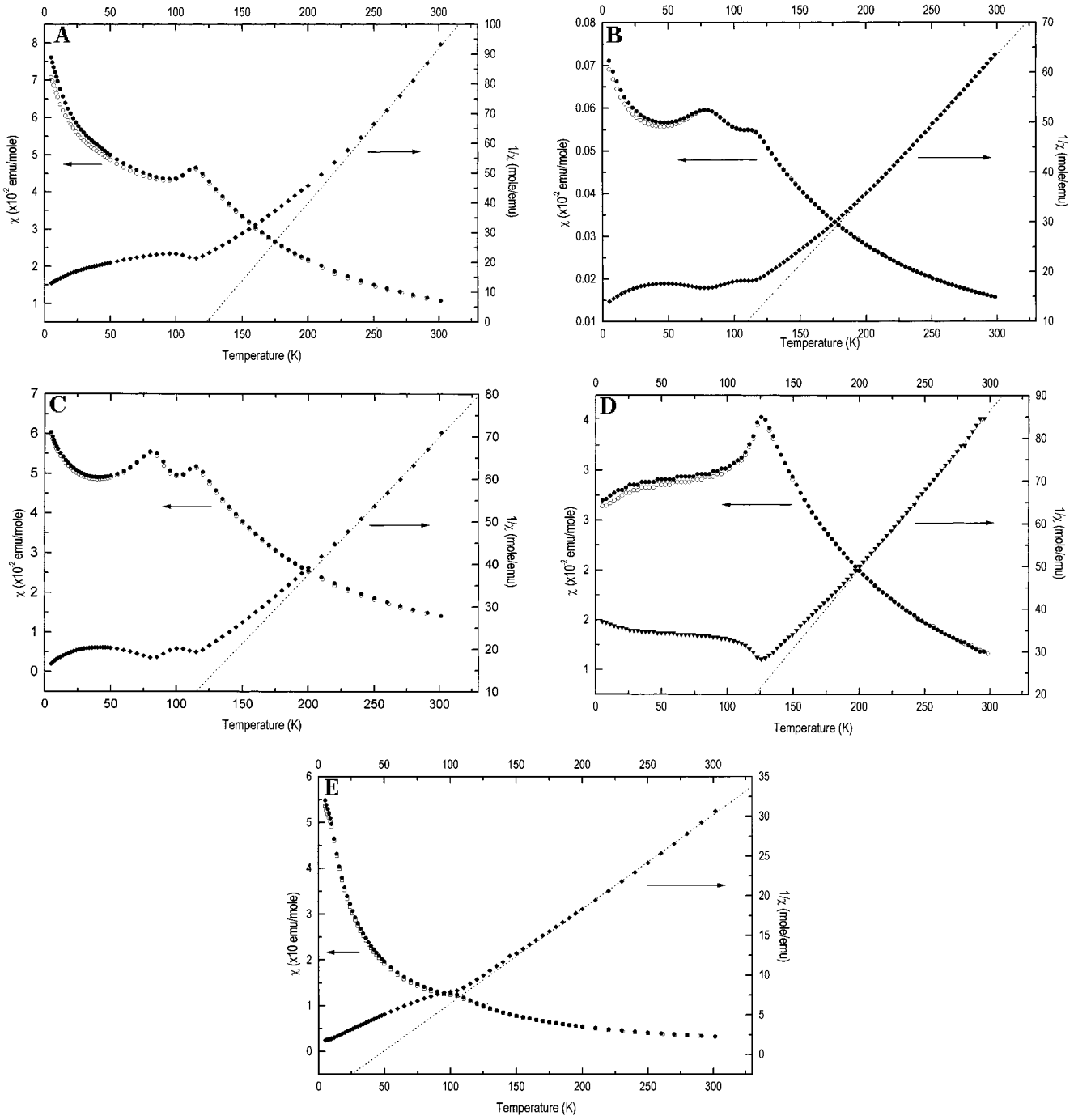

Figure 4. Magnetic data of $LnSrMn_{0.5}Ni_{0.5}O_4$: Ln = (A) La, (B) Pr, (C) Nd, (D) Sm, and (E) Gd. The FC and ZFC data are shown as filled and open circles, respectively. The Curie−Weiss fit results are shown as dotted lines.

Table 3. Important Bond Distances (Å) of $LnSrMn_{0.5}Ni_{0.5}O_4$ (Ln = La, Pr, Nd) from Rietveld Refinements of Room Temperature Neutron Diffraction Patterns

bond type	La	Pr	Nd
Ln/Sr−O1 × 4	2.604(1)	2.589(1)	2.582(1)
Ln/Sr−O2 × 1	2.441(3)	2.388(3)	2.380(3)
Ln/Sr−O2 × 4	2.7336(4)	2.7207(4)	2.716(4)
Mn/Ni−O1 × 4	1.9193(1)	1.9086(1)	1.9054(1)
Mn/Ni−O2 × 2	2.084(2)	2.091(2)	2.085(3)

Table 4. Curie−Weiss Parameters for $LnSrMn_{0.5}Ni_{0.5}O_4$ (Ln = La, Pr, Nd, Sm, Gd)

	T_N (K)		effective magnetic moment	Weiss temp (K)	temp range (K)
compd	interlayer	intralayer			
La		115	3.92	123	250−300
Pr	78	111	5.28	78	230−300
Nd	80	116	4.97	84	230−300
Sm	20−60	126	4.64	67	210−300
Gd	10	105	8.21	46	180−300

tions both from the core electrons and sample container. However, the orders of magnitude smaller diamagnetic corrections did not improve the data, and the positive χ_{TIP} terms would make the lines more curved. Nonetheless, we have attempted to fit the higher temperature portions of the data to the Curie−Weiss law to get the parameters in Table 4. Therefore, the magnetic moments and Weiss temperatures in this table should be taken as the highest and lowest limits of the true values, respectively. At any rate, the positive Weiss tempera-

Table 5. Calculations of Paramagnetic Moments of $LnSrMn_{0.5}Ni_{0.5}O_4$ (Ln = La, Pr, Nd, Sm, Gd) for Various Electronic Structures

		electronic structure		
compd	spin value used	$Mn^{III}-Ni^{III}$(HS)	$Mn^{III}-Ni^{III}$(LS)	$Mn^{IV}-Ni^{II}$
La	spin-only	4.42	3.67	3.39
	experimental	4.5−5.1	3.7	3.3−3.9
Pr	spin-only	5.69	5.13	4.92
	experimental	5.7−6.2	5.1	4.8−5.3
Nd	spin-only	5.71	5.15	4.96
	experimental	5.8−6.2	5.1	4.8−5.4
Sm	spin-only	4.67	3.97	3.71
	experimental	4.8−5.3	4.0	3.9−4.2
Gd	spin-only	9.09	8.75	8.63
	experimental	9.1−9.4	8.8	8.7−8.9

tures from the Curie−Weiss fits indicate that there are internal ferromagnetic fields in the paramagnetic temperature regime probably due to partial Mn/Ni atomic ordering, which forms regions of ferromagnetic ordering (below). The progressively pronounced deviations from the Curie−Weiss law as the temperature approaches the ordering temperature can also be attributed to the ferromagnetic interactions.

The magnetic moment calculated for the La compound is 3.92 μ_B, smaller than those of Millburn et al. (4.41 μ_B) and of Ganguly et al. (6.03 μ_B). In their paper, comparing their magnetic moment with calculated spin-only values for some possible cases of electronic structures of Mn and Ni atoms, Millburn et al. found that $Mn^{III}-Ni^{III}$(HS) case gave the best agreement and, consequently, concluded that their compound had Ni^{III}-(HS). However, we would like to point out that comparison with the spin-only values cannot be realistic to determine the oxidation states of metal ions. Comparison with the maximum and minimum experimental data that include spin−orbit couplings and orbital contributions would be more reasonable. In Table 5, we list the calculated magnetic moments for various possible electronic structures for Mn and Ni atoms using the experimentally observed magnetic moment values from the literature. The best agreements with our experimental values are found in the $Mn^{IV}-Ni^{II}$ cases for the La, Pr, and Nd samples contrary to Millburn et al. Considering that the magnetic moments in Table 4 should be larger than the true values because of the curvatures in the $1/\chi$ vs T plots, the agreements can be even better if higher temperature data were included in the Curie−Weiss fits. The Curie−Weiss parameters for the Sm and Gd data do not seem to agree with any of the three models probably because of the complicated magnetic properties of Sm and the large magnetic contribution from Gd in addition to the lack of higher temperature data than 300 K.

The oxidation state assignments from the magnetic data were confirmed by the XANES spectroscopic studies on the samples. Figures 5 and 6 show normalized (panel A) and first differential (panel B) Mn and Ni K-edge XANES spectra, respectively, for our samples as well as for reference compounds. Regardless of the variation of Ln atoms, all the compounds display almost identical XANES, indicating that the coordination geometry around absorbing atoms is very similar. Among many fine structures, the position of 1s→3d transition, which is dipole forbidden but quadrupole allowed, has been used in determining the oxidation state of an absorbing atom.[17−19] We used Mn_2O_3 and MnO_2 as reference materials for +3 and +4 states, respectively. Both Mn_2O_3 and MnO_2 show two 1s→ 3d peaks labeled as A_1 and A_2, which are ascribed to electronic transitions to final states with t_{2g} and e_g symmetries, respectively. The position of A_1 is known as an indicator of the oxidation state.[20] This peak appears at 6539.5 eV for Mn^{III} and 6540.0 eV for Mn^{IV}. Similarly, our synthesized reference samples, $LaSrMnO_4$ (Mn^{III}) and Ca_2MnO_4 (Mn^{IV}), showed A_1 peaks at the same positions as those of Mn_2O_3 and MnO_2, respectively, proving the reliability of this method. Since all our samples exhibit A_1 peaks at 6540.0 eV (Table 6), Mn is at +4 state, confirming our assignment of the oxidation state for Mn from the magnetic data. The rest of fine structures are due to electronic transitions into bound or quasi-bound states and the multiple scattering. Since site symmetry and interatomic distances also affect the shape and the position of these peaks, it is not straightforward to determine oxidation states from them.

The exactly same arguments can be applied to the determination of Ni oxidation state in our samples. The 1s→ 3d transition positions for $LaMn_{0.5}Ni_{0.5}O_3$ and $LaSrNiO_4$ as Ni^{II} and Ni^{III} references were found at 8332.0 and 8332.9 eV, respectively, proving the relationship of approximately 1 eV shift per unit change in oxidation state. These values agree with those of NiO (8332.1 eV) and NiOOH (8333.0 eV) reported by Mansour et al.[21] Depending on Ln atoms, there is a slight variation in the peak position (Table 6). However, these values, in the range of 8331.8−8332.4 eV, are closer to those of $LaMn_{0.5}Ni_{0.5}O_3$ and NiO suggesting that the Ni oxidation state is +2. The reason for the slight variation of the peak position depending on Ln atom, contrary to the Mn case, appears to be related with the nature of the 1s→ 3d transition. The 3d state is composed of t_{2g} and e_g levels, and the former nonbonding level is not sensitive to the site symmetry and interatomic distances while the later antibonding level is sensitive to these factors. Therefore, A_1 peaks in the Mn spectra are to the t_{2g} levels, showing a constant value of transition energy, while the transitions in the Ni spectra are to

(17) Roe, A. L.; Schneider, D. J.; Mayer, R. J.; Pyrz, J. W.; Widom, J.; Que, L., Jr. *J. Am. Chem. Soc.* **1984**, *106*, 1676.
(18) Westre, T. E.; Kennepohl, P.; DeWitt, J. G.; Hedman, B.; Hodgson, K. O.; Solomon, E. I. *J. Am. Chem. Soc.* **1997**, *119*, 6297.
(19) Wong, J.; Lytle, F. W.; Messmer, R. P.; Maylotte, D. H. *Phys. Rev. B* **1984**, *30*, 5596.
(20) Liu, R. S.; Jang, L. Y.; Chen, J. M.; Tsai, Y. C.; Hwang, Y. D.; Liu, R. G. *J. Solid State Chem.* **1997**, *128*, 326.
(21) Mansour, A. N.; Melendres, C. A.; Pankuch, M.; Brizzolara, R. A. *J. Electrochem. Soc.* **1994**, *141*, L69.

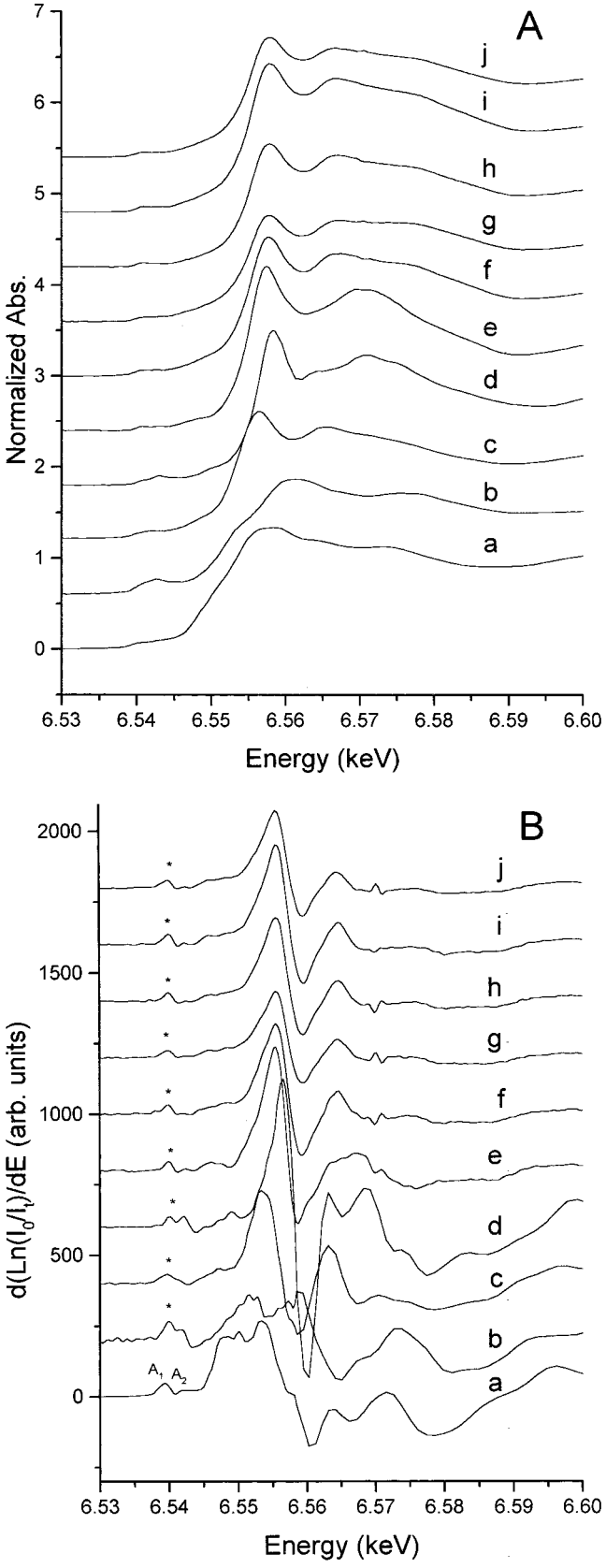

Figure 5. Normalized (panel A) and first differential (panel B) XANES spectra of Mn for (a) Mn_2O_3, (b) MnO_2, (c) $LaSrMnO_4$, (d) Ca_2MnO_4, (e) $LaMn_{0.5}Ni_{0.5}O_3$, (f) $LaSrMn_{0.5}Ni_{0.5}O_4$, (g) $PrSrMn_{0.5}Ni_{0.5}O_4$, (h) $NdSrMn_{0.5}Ni_{0.5}O_4$, (i) $SmSrMn_{0.5}Ni_{0.5}O_4$, and (j) $GdSrMn_{0.5}Ni_{0.5}O_4$. 1s→3d transition (A_1 peak) is labeled by an asterisk (∗).

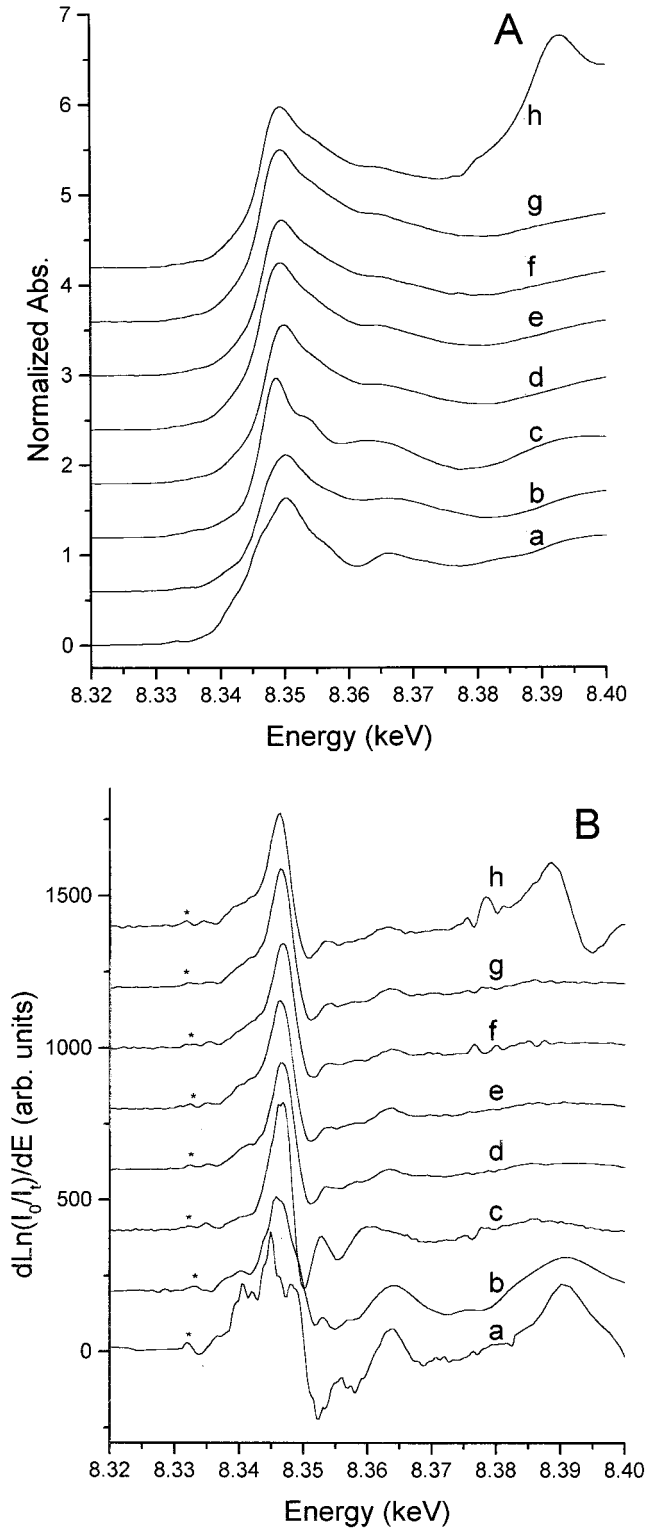

Figure 6. Normalized (panel A) and first differential (panel B) XANES spectra of Ni for (a) NiO, (b) $LaSrNiO_4$, (c) $LaMn_{0.5}Ni_{0.5}O_4$, (d) $LaSrMn_{0.5}Ni_{0.5}O_4$, (e) $PrSrMn_{0.5}Ni_{0.5}O_4$, (f) $NdSrMn_{0.5}Ni_{0.5}O_4$, (g) $SmSrMn_{0.5}Ni_{0.5}O_4$, and (h) $GdSrMn_{0.5}Ni_{0.5}O_4$. 1s→3d transition (A_1 peak) is labeled by an asterisk (∗).

the e_g levels, showing dependency on Ln atom. Alternatively, the variation may be because of partial oxidation of Ni atoms by interstitial oxygen, which is common in Ni^{II} compounds of this structure type.[22] The gradual shift of the peak position to lower energy as the size of

(22) (a) Rice, D. E.; Buttrey, D. J. *J. Solid State Chem.* **1993**, *105*, 197. (b) Jorgensen, J. D.; Dabrowski, B.; Pei, S.; Hinks, D. G. *Phys. Rev. B* **1989**, *40*, 2187.

Table 6. 1s→3d Transition Energies of Mn and Ni Atoms in $LnSrMn_{0.5}Ni_{0.5}O_4$ Compounds

compd	Mn K-edge energy[a,b]	Ni K-edge energy[a]
Mn_2O_3[c]	6539.5	
MnO_2[c]	6540.0	
$LaSrMnO_4$[c]	6539.5	
Ca_2MnO_4[c]	6540.0	
$LaMn_{0.5}Ni_{0.5}O_3$[c]	6539.9	8332.0
$LaSrMn_{0.5}Ni_{0.5}O_4$	6540.0	8332.4
$PrSrMn_{0.5}Ni_{0.5}O_4$	6540.0	8332.4
$NdSrMn_{0.5}Ni_{0.5}O_4$	6540.0	8332.3
$SmSrMn_{0.5}Ni_{0.5}O_4$	6540.0	8332.1
$GdSrMn_{0.5}Ni_{0.5}O_4$	6540.0	8331.8
NiO[c]		8332.1
$LaSrNiO_4$[c]		8332.9
NiOOH[c,d]		8333.0

[a] Energy measured as the inflection position of 1s→ 3d transition. [b] Position of the A_1 peak (see text). [c] Reference compounds. [d] Taken from ref 21.

Ln decreases may be understood in terms of this interstitial oxygen, i.e., as the lattice dimension becomes smaller with smaller Ln atoms there is smaller room for interstitial oxygen atoms to oxidize Ni. The latter interpretation leads us to consider a mixed oxidation state of Ni^{II} and Ni^{III}, especially for those with large Ln atoms. Following the discussion of Millburn et al., these Ni^{III} are likely to be high spin, which may be responsible for the larger experimental magnetic moments than the theoretical values as discussed above.

It is not certain why the compounds from lower temperature preparations in the literature gave larger magnetic moment values than ours. But it is highly likely that the different degree of Mn and Ni distributions depending on the synthesis temperature is responsible. Interestingly, the oxidation states of Mn and Ni in the perovskite $LaMn_{0.5}Ni_{0.5}O_3$ compound appear to depend on the synthesis route also. Therefore, while those from the high-temperature solid-state method are reported to have Mn^{IV} and Ni^{II},[1,6,7] those from low-temperature precursor routes are reported to have Mn^{III} and Ni^{III}.[10] Although our synthesis temperature is only 100−200 °C higher than those of the literature, the difference may be significant enough to induce such a drastic change of electronic structure.

The temperature-dependent ZFC and FC magnetic susceptibility data for our $LaSrMn_{0.5}Ni_{0.5}O_4$ sample qualitatively agree with those of Millburn et al. There is a local maximum indicating an antiferromagnetic ordering at about 115 K. The magnetization increases as the temperature is decreased, and the ZFC and FC data diverge from each other below this temperature (T_N). In the paper of Millburn et al., the magnetization data for $LaSrMn_{0.5}Ni_{0.5}O_4$ from a 1200 °C reaction showed a T_N at 75−80 K, and the ZFC and FC data diverged below this temperature. The 1300 °C annealing raised T_N to 88−93 K and reduced the divergence between ZFC and FC data. By fitting to the Curie−Weiss law, they obtained positive Weiss temperatures of 68 and 75 K for the 1200 and 1300 °C samples, respectively, lower than our 123 K. They explained the magnetic behavior by supposing that a part of the spins was frozen or antiferromagnetically ordered below T_N responsible for the local maximum while the other part showed spin-glass-like behavior responsible for the ZFC and FC divergence and the increase of magnetization on cooling. This explanation appears to hold for our compounds. The variation of the magnetic properties with thermal history was explained with the different Mn and Ni distribution to result in different proportions of frozen and spin-glass-like parts of the spins. Following this discussion, the data of our 1400 °C sample can be understood as having more homogeneous Mn and Ni distribution increasing the proportion of the spins that can undergo antiferromagnetic ordering to result in higher T_N and Weiss temperature.

Taking our assignment of oxidation states of Mn^{IV} and Ni^{II} from the Curie−Weiss fits and the XANES data, the nearest neighbor magnetic interactions in the MO_2 layer can be understood in terms of the superexchange model. According to the Goodenough's rule, the Ni^{II}−Ni^{II} (d^8−d^8) and Mn^{IV}−Mn^{IV} (d^3−d^3) interactions through 180° M−O−M bonds are antiferromagnetic while the Mn^{IV}−Ni^{II} interactions are ferromagnetic.[23] Although we did not observe any evidence of Mn/Ni ordering by neutron diffraction studies, it is likely that these atoms are locally ordered to form regions in which Mn and Ni atoms interact ferromagnetically as in superparamagnetic clusters because of their charge difference. The ferromagnetism of $LaMn_{0.5}Ni_{0.5}O_3$ is explained by this superexchange mechanism although there is no evidence for Mn/Ni ordering.[1] It appears that the charge difference by two units may not be a strong driving force to order Mn^{IV} and Ni^{II} ions. However, the similar ferromagnetic $LaMn_{0.5}Cu_{0.5}O_3$ is reported to have a superstructure probably because Cu^{II} is a Jahn−Teller ion in addition to the charge difference.[24] This comparison suggests that the Mn^{IV} and Ni^{II} ions can order, at least locally. The 2D structure of our $LnSrMn_{0.5}Ni_{0.5}O_4$ compounds may have a less favorable driving force to order Mn^{IV} and Ni^{II} ions than the perovskites, but still it is possible to have local ordering. The ferromagnetic field in the paramagnetic data can be understood by these Mn/Ni-ordered regions. The overall antiferromagnetic behavior is probably due to the Ni^{II}−Ni^{II} and Mn^{IV}−Mn^{IV} junctions between the ferromagnetic regions as well as the regions where the Ni^{II}−Ni^{II} and Mn^{IV}−Mn^{IV} arrangements dominate. Therefore, depending on the local distribution of Mn and Ni atoms, the nature of the overall magnetic interactions can be changed. The variations of T_N and Weiss temperature of the La compound with the thermal history can be understood as the increase of the size of the ferromagnetic region with the increase of the reaction temperature. However, because our compounds are inherently inhomogeneous in Mn/Ni distribution, there must be frustrated spins that are not involved in the ferromagnetic regions clusters, and these frustrated spins are likely the cause of the discrepancies of the FC and ZFC data at low temperatures. While most of the literature examples of superparamagnetic clusters are considered to be dynamic in nature changing the coherence lengths with temperature and drifting in space,[25] the sort of superparamagnetic clusters in the present compounds are localized because the Mn and Ni distribution and

(23) Goodenough, J. B. *Magnetism and the Chemical Bonds*; John Wiley and Sons: New York, 1963; pp 168−183.
(24) Anderson, M. T.; Greenwood, K. B.; Taylor, G. A.; Poeppelmeier, K. R. *Prog. Solid State Chem.* **1993**, *22*, 197.
(25) Battle, P. D.; Blundell, S. J.; Green, M. A.; Hayes, W.; Honold, M.; Klehe, A. K.; Laskey, N. S.; Millburn, J. E.; Murphy, L.; Rosseinsky, M. J.; Samarin, N. A.; Singleton, J.; Sluchanko, N. E.; Sullivan, S. P.; Vente, J. F. *J. Phys.: Condens. Matter* **1996**, *8*, L427.

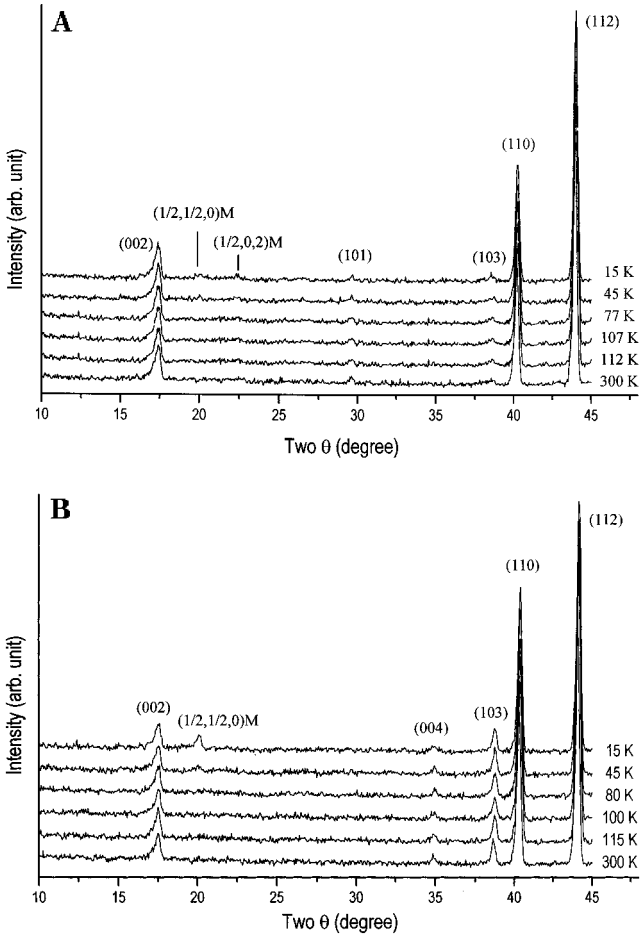

Figure 7. Temperature variations of the neutron diffraction patterns of $LnSrMn_{0.5}Ni_{0.5}O_4$: Ln = (a) Pr and (b) Nd.

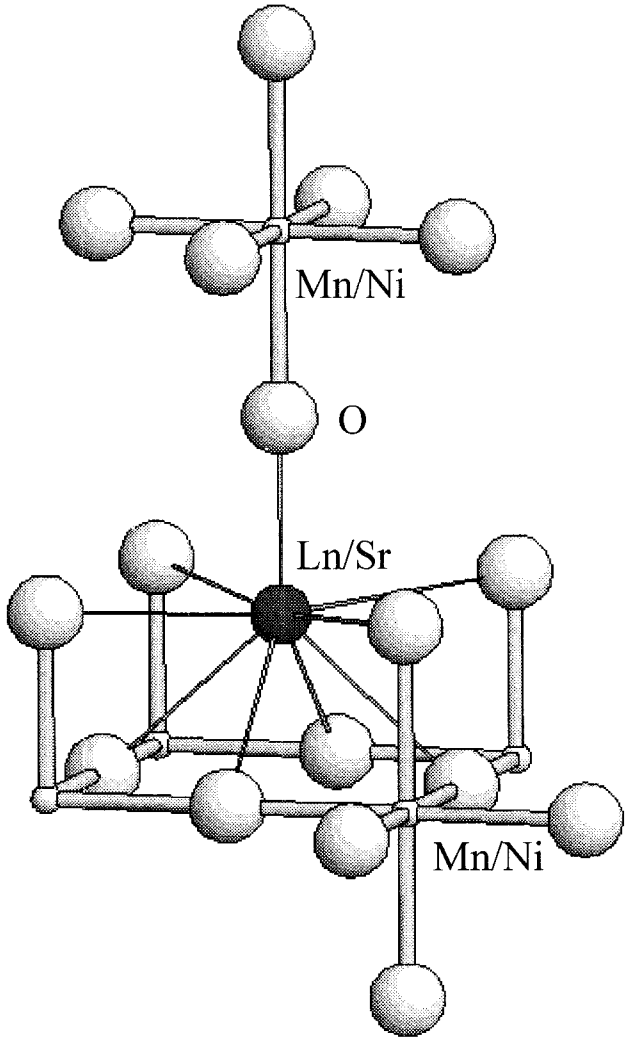

Figure 8. Local environment around a Ln atom in $LnSrMn_{0.5}Ni_{0.5}O_4$ structure.

locations cannot be changed with temperature at low temperatures.

The Pr and Nd compounds show additional features to the La compound. There are two local maxima in the χ vs temperature plots (Figure 4). The higher temperature ones appear to have the same origin as the one in the La compound, that is, due to the AF ordering between ferromagnetic regions in the MO_2 layers. The lower temperature maxima that were absent in the La compound should be due to the different magnetic properties between La and Pr/Nd atoms. Low-temperature neutron diffraction data of the samples also show that the Pr and Nd samples have additional magnetic interactions at low temperatures that are absent in the La compound (Figure 7). The neutron diffraction patterns of the Nd compound down to 80 K are identical to that at 300 K except for the peak position shifts because of thermal expansion. However, a peak at $2\theta = 19.64°$ ($d = 5.38$ Å) develops at around 45 K whose intensity increases on cooling. This peak can be indexed as (1/2,1/2,0) based on the chemical unit cell indicating an antiferromagnetic ordering. In the Pr sample, two very weak magnetic peaks start to grow from 45 K and downward at $2\theta = 19.62°$ ($d = 5.38$ Å) and 21.97° ($d = 4.81$ Å) that can be indexed as (1/2,1/2,0) and (1/2,0,2), respectively. We were unable to explain the magnetic peak with any models we have tried mainly because of the limited magnetic data available. However, it is evident that there are additional magnetic interactions at 78 and 80 K for the Pr and Nd compounds. The neutron diffraction data for the La compound do not show any magnetic peaks down to 15 K.

One can consider two possibilities for the Pr(Nd) atoms to order magnetically; ordering of Pr(Nd) atoms among themselves and ordering with the Mn/Ni atoms in the neighboring MO_2 layers. The first possibility can be ruled out because the ordering temperatures of 78 and 80 K are much higher than any of the reported ordering temperatures in rare earth oxides and there is no report on Pr/Nd magnetic ordering in other related layered compounds.[26] For the second type of interaction, we can express the magnetic exchange Hamiltonian as $H = JS_M \cdot S_{Ln}$ where J is the coupling constant and S_M and S_{Ln} are spin operators of M (Mn/Ni) and Ln atoms, respectively. Since the Ln atoms are between two MO_2 layers, each Ln atom can interact with the M atoms of both layers. There are nine oxygen atoms bonded to each Ln atom, one with a 180° M−O−Ln bond angle to the upper MO_2 layer while the other eight with close to 90° bond angles to the lower layer (Figure 8). The 90° and 180° bond angles typically result in the opposite signs of J values. Although the details of the interactions are

(26) Samsonov, G. V., Ed. *The Oxide Handbook*, 2nd ed.; IFI/Plenum: New York, 1982; p 211.

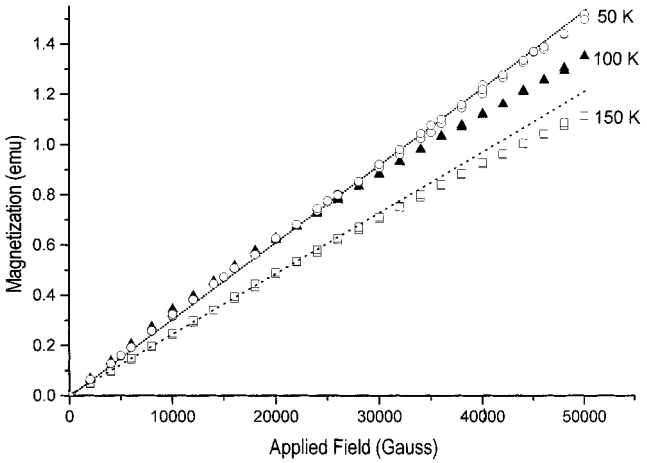

Figure 9. Field-dependent magnetization data of $NdSrMn_{0.5}Ni_{0.5}O_4$ taken at various temperatures.

not available, we can consider that the interactions to the M atoms in the upper and the lower layers have different signs to align the M spins of adjacent layers antiparallel. In the La compound case, because S_{Ln} is zero, there is no interlayer interaction leaving each layer almost independent to one another. In the Pr and Nd cases, because the S_{Ln} is nonzero, the M spins of adjacent layers order antiferromagnetically to give the low-temperature antiferromagnetic interactions. Moreover, since they have the similar magnetic moments and ionic sizes, their J and S_{Ln} values will be close to each other to give similar T_N values. To our knowledge, there is no literature data that show interlayer magnetic interactions mediated by Ln atoms as ours. However, we would like to point out that most of the layered compounds reported are either paramagnetic or antiferromagnetic, which are not suitable to exhibit the above suggested cooperative M−O−Ln−O−M interactions. Since there are four equivalent M atoms in the lower layer of Figure 8 interacting with a Ln atom, these have to order ferromagnetically among themselves in order to yield a nonfrustrated Ln moment. Therefore, the presence of the aforementioned ferromagnetic regions clusters within the MO_2 layer seems to be a prerequisite to exhibit the interlayer antiferromagnetic ordering as in our Pr and Nd samples.

Field-dependent magnetization data for the Nd compound at 50, 100, and 150 K shown in Figure 9 show slight deviations from linearity. The deviation in the 150 K data can be explained with the ferromagnetic regions. Millburn et al. explained the similar deviations below T_N with the spin-glass-like nature of their $LaSrMn_{0.5}Ni_{0.5}O_4$ compound. The degree of deviation increased as the temperature was lowered. However, in our Nd compound, the deviation in the 50 K data is smaller than that of the 100 K data, which cannot be explained with the spin-glass model alone. Alternatively, the different field dependency at the three temperatures can be explained with the motion of the ferromagnetic regions. As the temperature is lowered across the higher T_N (intralayer), the ferromagnetic regions are partly frozen or ordered antiferromagnetically in the MO_2 layers reducing their freedom of motion to give the nonlinearity in the M(H) behavior. Upon further cooling below the lower T_N (interlayer), the ferromagnetic regions are almost completely frozen across the layers reducing the nonlinearity in the M(H) behavior.

The proposed interlayer magnetic interaction mechanism may be applied to the CMR $Ln_{1.4}Sr_{1.6}Mn_2O_7$ compounds with the $n = 2$ structure of the Ruddelsden−Popper series.[27] The long-range ferromagnetic ordering of the La compound is suppressed by substitutions with Pr or Nd to result in short-range ordering and much reduced magnetic moments. Thus far, the reason for the breakdown of the long-range ordering is understood as due to the increased Jahn−Teller distortions of the MnO_6 octahedra by the Pr and Nd substitutions. In addition to this mechanism, the short-range ordering may result from the competition between the double-exchange-driven ferromagnetic interaction and above proposed antiferromagnetic interaction including the rare earth ions between the Mn_2O_7 layers. The Pr and Nd atoms can induce antiferromagnetic interactions because there is already ferromagnetic interactions within the Mn_2O_7 layers.

The Sm compound shows yet different magnetic behavior (Figure 4). In contrast to the other compounds, the magnetization decreases on cooling. Despite that Sm has a nonzero magnetic moment, there is only one local maximum in the χ vs temperature plot. However, the broad hump in the temperature range 20−60 K might be due to the weak interlayer magnetic interactions. The almost constant gap between the divergent ZFC and FC data passing through this temperature range while in the La compound the gap increasing on cooling also may be evidence for the weak interlayer interaction. The decreasing magnetization on cooling appears to be due to the decrease of Sm^{3+} magnetic moment. The first excited state with $J = 7/2$ of Sm^{3+} is so close to the ground state with $J = 5/2$ that depopulation of the excited state on cooling lowers the Sm part of magnetization to more than offset the increase of the Mn/Ni magnetization. The Gd moment dominates the magnetic data of the Gd compound (Figure 4). There is a cusp at 105 K in the magnetization plot, indicating an antiferromagnetic ordering within the MO_2 layer. There also is a very weak inflection point at about 10 K that may be due to the interlayer interactions.

The reduced interlayer T_N values of Sm and Gd compounds from those of Pr and Nd compounds appear to be related with many factors. First, the smaller ionic sizes of Sm and Gd than those of Pr and Nd may be responsible. The Ln−O (Ln = Sm, Gd) distances will be larger than are required by the bond valences of Ln^{3+} ions because they are mixed with much larger Sr^{2+} ions. Bond valence decreases exponentially with bond distance; therefore, small differences in ionic size may cause significant changes of J and, thus, T_N. Second, the electronic structure of Ln^{3+} ions may also be responsible. Pr^{3+} (f^2) and Nd^{3+} (f^3) ions have unpaired electrons in less than half of the f-orbitals, while Sm^{3+} (f^5) and Gd^{3+}(f^7) have unpaired electrons in more than half of the f-orbitals. Therefore, the unpaired electrons of Pr^{3+} and Nd^{3+} ions lie on the lower levels while some of the electrons of Sm^{3+} and Gd^{3+} are on the upper levels of the crystal field split f-orbitals. Reflecting that the magnetic interactions between transition metal ions strongly depend on the electronic structures of the metal

(27) Hur, N. H.; Kim, J.-T.; Yoo, K. H.; Park, Y. K.; Park, J.-C.; Chi, E. O.; Kwon, Y.-U. *Phys. Rev. B* **1998**, *57*, 10740.

ions, for instance, in the octahedral field, whether there are unpaired electron in t_{2g} and/or e_g levels, the similar argument may be applied to the f-element cases. Thus the interlayer magnetic interactions mediated by the Ln moments are different between Pr/Nd and Sm/Gd cases in both type and strength.

In conclusion, we have synthesized new K_2NiF_4 type $LnSrMn_{0.5}Ni_{0.5}O_4$ (Ln = La, Pr, Nd, Sm, Gd) compounds and studied their magnetic properties. The magnetic properties of the La compound can be characterized with the antiferromagnetic interaction between localized ferromagnetically ordered regions due to partial ordering of Mn/Ni atoms and with frustrated spins of Mn/Ni disordered regions. The other compounds with other Ln atoms show additional magnetic interactions at lower temperatures. For these, a magnetic interaction mechanism that involves the ferromagnetic regions in the MO_2 layers and the Ln ions is proposed. This mechanism can be applied to the layered colossal magnetoresistant $Ln_{1+x}Sr_{2-x}Mn_2O_7$ materials to explain the drastic variation of the physical properties depending on the nature of Ln atoms.

Acknowledgment. Financial support from the Korea Science and Engineering Foundation (KOSEF-971-0306-050-3) and the Ministry of Education (BSRI-97-3421) are gratefully acknowledged. The neutron diffraction experiment was performed at HRPD operated under the Nuclear R & D program by MOST, Korea. We thank Dr. Y. S. Kim at Korea Basic Science Institute for the magnetic measurements.

CM990098K